Journal of Superconductivity and Novel Magnetism (2019) 32:2185–2192
https://doi.org/10.1007/s10948-018-4948-5

ORIGINAL PAPER

Electronic Structures and Ferromagnetic Properties of 3d (Cr)-Doped BaSe Barium Selenide

Hocine Bahloul[1] · Allel Mokaddem[2] · Bendouma Doumi[3] · Mohamed Berber[2] · Abdelkader Boudali[1]

Received: 10 September 2018 / Accepted: 13 November 2018 / Published online: 19 November 2018

Abstract

In this study, we have employed the first-principle methods based on spin-polarized density functional theory to investigate the structural parameters, the electronic structures, and the half-metallic ferromagnetic behavior of chromium (Cr)-doped barium selenide (BaSe) such as $Ba_{1-x}Cr_xSe$ at concentrations $x = 0.25$, 0.5, and 0.75. The exchange and correlation potential is described by the generalized gradient approximation of Wu and Cohen (GGA-WC). The calculated structural parameters of BaSe are in good agreement with theoretical data. Our findings reveal that the p-d exchange coupling is ferromagnetic for $Ba_{0.75}Cr_{0.25}Se$ and $Ba_{0.5}Cr_{0.5}S$, but it becomes anti-ferromagnetic for $Ba_{0.25}Cr_{0.75}S$. The electronic structures exhibit that the $Ba_{1-x}Cr_xSe$ materials for all concentrations are half-metallic ferromagnets with spin polarization of 100% and total magnetic moment per Cr atom of 4 μ_B. Therefore, the $Ba_{1-x}Cr_xSe$ compounds are suitable candidates for possible spintronics applications.

Keywords DFT · Electronic structures · Half-metallic ferromagnetic · Cr-doped BaSe

1 Introduction

In recent years, the experimental and theoretical researches on the II–V and III–V semiconductors doped with transition metals have attracted much attention because these materials have interesting electronic and magnetic properties and due to their remarkable use as fundamental materials for diluted magnetic semiconductors (DMS). The DMS based on the II–V and III–V semiconductors are considered potential candidates for modern spintronics applications because they show stability in the ferromagnetic ordering configuration and they exhibit a half-metallic ferromagnetic behavior [1–7]. Spin-based electronics or spintronics is modern field of research exploiting the electron spin plus its charge as a second-degree freedom to improve the processing performance and data storage of spin-based devices. The expected advantage of spintronic devices over the conventional electronic ones would be nonvolatility, increased data processing speed, increased transistor density, and decreased power consumption [8]. Several experimental and theoretical investigations have been performed on the half-metallic and magnetic properties of DMS based on III–V and II–VI semiconductors such as the Mn-doped InSb [9], the Mn-doped AlSb [10], the V doped AlSb [11], the Mn-doped GaAs [12], the theory of ferromagnetic (III, Mn)V semiconductors [13], the Ni-doped ZnS [14], Fe-doped ZnS [15], the (C, Fe)-doped CdSe [16], the V-doped ZnS [17], the V-doped BaS [18], and the V-doped SrO [19].

To the best of our knowledge and according to researches available in the literature, there are no experimental and theoretical studies on magnetic and electronic properties of Cr-doped Barium selenide (BaSe)-based DMS. In this study, we have performed the structural, electronic, and ferromagnetic properties of $Ba_{1-x}Cr_xSe$ at various concentrations $x = 0.25$, 0.5, and 0.75. We have used in our prediction the full potential linearized augmented plane wave (FP-LAPW) method within density functional theory (DFT) [20], where the exchange and correlation potential is described by the generalized gradient approximation of Wu and Cohen (GGA-WC) [21].

✉ Hocine Bahloul
bahloul.houcine60@gmail.com

✉ Allel Mokaddem
mokaddem.allel@gmail.com

✉ Bendouma Doumi
bdoummi@yahoo.fr

[1] Laboratory of Physico-Chemical Studies, University of Saida, 20000 Saida, Algeria

[2] Centre Universitaire Nour Bachir El Bayadh, 32000 El Bayadh, Algeria

[3] Faculty of Sciences, Department of Physics, Dr. Tahar Moulay University of Saida, 20000 Saida, Algeria

2 Method of Calculations

We have used the full-potential linearized augmented plane-wave (FP-LAPW) method within the framework of the DFT [20] as implemented in WIEN2K package [22]. We have treated the exchange and correlation potential by the generalized gradient approximation of Wu and Cohen (GGA-WC) [21] to compute structural, electronic, and ferromagnetic properties of $Ba_{1-x}Cr_xSe$ at different concentrations $x = 0.25$, 0.5, and 0.75 of chromium (Cr) impurity. We have taken $K_{max} = 9.0/R_{MT}$, where the K_{max} is the size of the largest K vector of the plane wave and the R_{MT} are the averages radii of muffin-tin spheres of Ba, Se, and Cr atoms. The charge density was Fourier expanded up to $G_{max} = 14$ (a.u.)$^{-1}$, where G_{max} is the largest vector in the Fourier expansion, and the maximum partial waves within the atomic sphere was $l_{max} = 10$. The cutoff energy was set to −6 Ryd to separate core and valence states. We have employed the Monkhorst–Pack mesh [23, 24] of the $(4 \times 4 \times 4)$ k-points for BaSe, $Ba_{0.75}Cr_{0.25}Se$, and $Ba_{0.25}Cr_{0.75}Se$ and the $(4 \times 4 \times 3)$ k-points for $Ba_{0.5}Cr_{0.5}Se$ in the Brillouin-zone integration. Self-consistency was reached when the total energy convergence was set at 0.1 mRy.

3 Results and Discussions

3.1 Structural Properties

BaSe was made in 1925 by reducing the $BaSeO_3$ with hydrogen at a red heat [25]. The BaSe is one of IIA–VI alkaline-earth chalcogenide group, crystallizing in a rock-salt NaCl (B1) phase with space group of $Fm\bar{3}m$ No. 225. The conventional structure of BaSe has two types of atoms Ba and Se, which are located respectively at (0, 0, 0) and (0.5, 0.5, 0.5) sites. We have created the $Ba_{1-x}Cr_xSe$ supercells of 8 atoms such as the Ba_3CrSe_4 for concentration $x = 0.25$, the $Ba_2Cr_2Se_4$ for $x = 0.5$, and the $BaCr_3Se_4$ for $x = 0.75$ by substituting of one, two, and three Cr atoms at Ba sites, respectively. The $Ba_{0.75}Cr_{0.25}Se$ and $Ba_{0.25}Cr_{0.75}Se$ supercells have a cubic structure with space group of $Pm\bar{3}m$ No. 221, while the $Ba_{0.5}Cr_{0.5}Se$ has a tetragonal structure with space group of $P4/mmm$ No. 123. We have noted that our $Ba_{0.75}Cr_{0.25}Se$, $Ba_{0.5}Cr_{0.5}Se$ and $Ba_{0.25}Cr_{0.75}Se$ structures are described by the supercells completely free from defects, but the real supercells my necessarily have side effects like defects. However, our predictions are valid only for better calculations of supercells close to the ordered stoichiometric structures of $Ba_{0.75}Cr_{0.25}Se$, $Ba_{0.5}Cr_{0.5}Se$, and $Ba_{0.25}Cr_{0.75}Se$ compounds. We hope that our investigations of novel electronic and ferromagnetic properties of $Ba_{1-x}Cr_xSe$ provide predictions for experimentalists to explore these new materials for practical spintronics applications in the future.

We have calculated the formation energies to verify the solid state stability of Ba_3CrSe_4, $Ba_2Cr_2Se_4$ and $BaCr_3Se_4$ compounds in the rock-salt NaCl (B1) structure. The formation energies (E_{form}) of the $Ba_{4-y}Cr_ySe_4$ doping systems are determined by using the following expression [26, 27]:

$$E_{form} = E_{total}\left(Ba_{4-y}Cr_ySe_4\right) - \frac{(4-y)E(Ba)}{8} - \frac{yE(Cr)}{8} - \frac{4E(Se)}{8} \quad (1)$$

where the $E_{total}(Ba_{4-y}Cr_ySe_4)$ is minimum total energy of $Ba_{4-y}Cr_ySe_4$ per atom and the E(Ba), E(Cr), and E(Se) are respectively the minimum total energies per atom of bulks Ba, Cr, and Se, and the $y = 1$, 2, and 3 are the number of substitute Cr atoms in $Ba_{4-y}Cr_ySe_4$ supercells. We have found that the formation energies are −4.5, −4.83, and −5.34 eV for Ba_3CrSe_4, $Ba_2Cr_2Se_4$, and $BaCr_3Se_4$, respectively. Consequently, the negative formation energies mean that our compounds are thermodynamically stable in the ferromagnetic rock-salt phase.

We have performed the optimization of BaSe and $Ba_{1-x}Cr_xSe$ at various concentrations by the fitting of Murnaghan's equation of state [28] that reveals the variation of the total energy as a function of volume. Table 1 summarizes the predicted structural parameters of our compounds such as the lattice constants (a), bulk modules (B), and their pressure derivatives (B') with other theoretical [29–33] and experimental data [34–36] for comparison purposes. The

Table 1 Calculated lattice constant (a), bulk modulus (B), and its pressure derivative (B') for BaSe and $Ba_{1-x}Cr_xSe$ at concentrations $x = 0.25$, 0.5, and 0.75

Compound	a (Å)	B (GPa)	B'	Method
This work				GGA-WC
BaSe	6.550	38.701	4.639	
	6.345	41.090	4.690	
$Ba_{0.75}Cr_{0.25}Se$				
	6.078	46.629	4.656	
$Ba_{0.5}Cr_{0.5}Se$				
	5.732	57.325	4.105	
$Ba_{0.25}Cr_{0.75}Se$				
Other calculations				
BaSe	6.563 [29]	40.89 [29]	4.534 [29]	GGA-WC
	6.561 [30]	38.667 [30]	6.561 [30]	GGA-WC
	6.563 [31]	40.89 [31]	3.781 [31]	GGA-WC
	6.668 [32]	34.00 [32]	5.06 [32]	GGA-PBE
	6.66 [33]			GGA-PBE
	6.593 ± 0.016 [34] 6.600 [35]	43.4 ± 2.6 [36]		Experimental

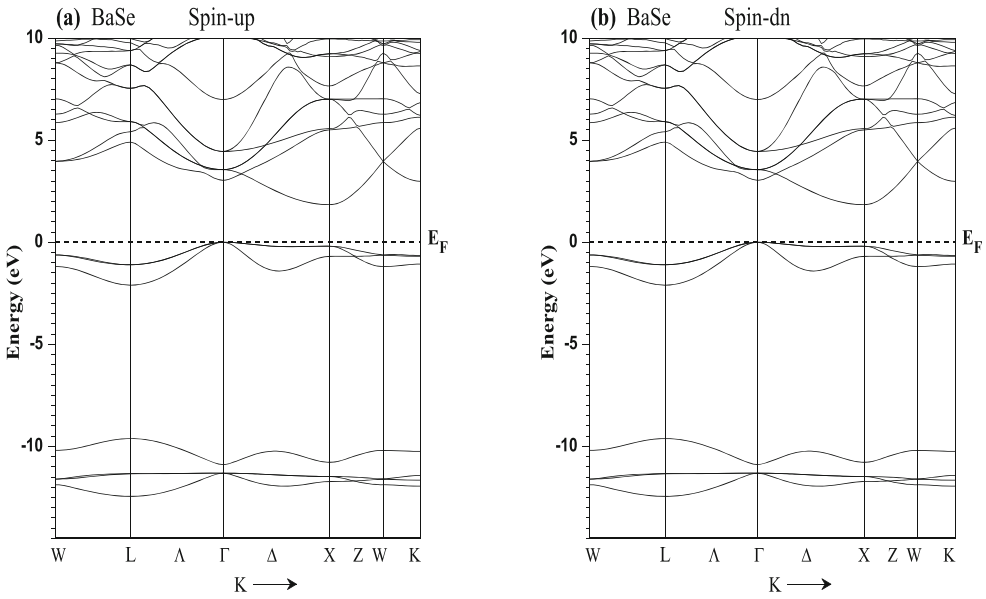

Fig. 1 Spin-polarized band structures for BaSe. **a** Majority spin (up) and **b** minority spin (dn). The Fermi level is set to zero (horizontal dotted line)

results of *a* and *B* for BaSe show the good agreement compared to experimental values [34–36] and the theoretical calculations [29–31] found by the use of the same GGA-WC approximation [21]. Owing to better performance of GGA-WC potential for structural properties, our calculations of structural parameters *a* and *B* of BaSe are improved with respect to the theoretical values [32, 33] found by the generalized gradient approximation of Perdew-Burke-Ernzerhof (GGA-PBE) [37]. For the $Ba_{1-x}Cr_xSe$ doping structures, the difference between the ionic radii of Ba atom and the substituted Cr impurity leads to the decrease of the lattice constant as the Cr concentration increases. There are no realized studies on the structural parameters of the $Ba_{1-x}Cr_xSe$ doping compounds in order to compare them with our results.

3.2 Electronic Structures, Half-Metallic Behavior, and Magnetic Properties

The electronic structures of BaSe and $Ba_{1-x}Cr_xSe$ such as the spin-polarized band structures and densities of states have predicted by using the theoretical optimized lattice constants. The band structures of BaSe, $Ba_{0.75}Cr_{0.25}Se$, $Ba_{0.5}Cr_{0.5}Se$, and $Ba_{0.25}Cr_{0.75}Se$ are presented in Figs. 1, 2, 3, and 4, respectively. Figure 1 depicts that spin up and spin down of BaSe exhibit similar semiconductor band structures with an indirect band gap ($E^{\Gamma-X}$) of 1.843 eV, which occurs between the Γ and X high symmetry points. Figures 2, 3, and 4 of $Ba_{0.75}Cr_{0.25}Se$, $Ba_{0.5}Cr_{0.5}Se$, and $Ba_{0.25}Cr_{0.75}Se$ reveal a half-metallic character, resulting

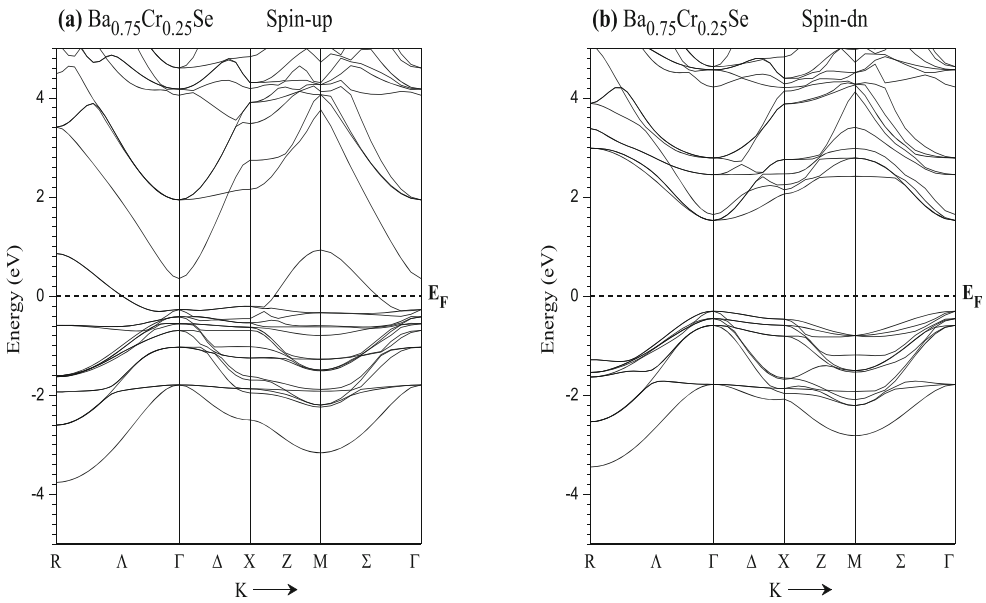

Fig. 2 Spin-polarized band structures for $Ba_{0.75}Cr_{0.25}Se$. **a** Majority spin (up) and **b** minority spin (dn). The Fermi level is set to zero (horizontal dotted line)

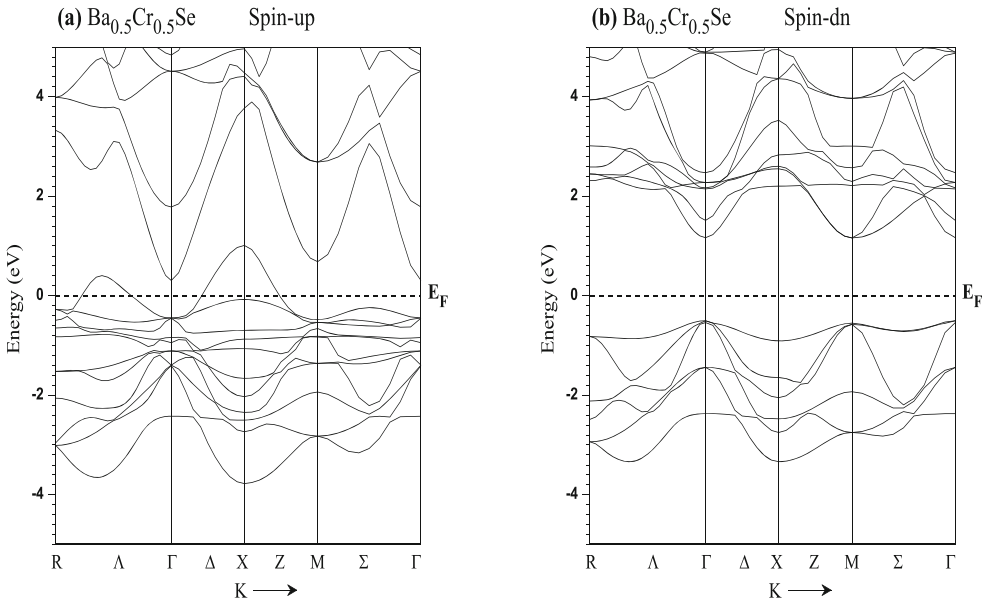

Fig. 3 Spin-polarized band structures for $Ba_{0.5}Cr_{0.5}Se$. **a** Majority spin (up) and **b** minority spin (dn). The Fermi level is set to zero (horizontal dotted line)

from metallic and semiconductor natures of majority-spin bands and minority-spin bands, respectively. The majority-spin bands of $Ba_{1-x}Cr_xSe$ doping compounds have direct half-metallic ferromagnetic gaps situated at Γ high symmetry point. The $Ba_{0.75}Cr_{0.25}Se$, $Ba_{0.5}Cr_{0.5}Se$, and $Ba_{0.25}Cr_{0.75}Se$ compounds have half-metallic ferromagnetic gaps of 1.832, 1.668, and 1.084 eV, respectively. On the other hand, the majority-spin bands show a half-metallic gap (G_{HM}), which is defined as the minimum of the lowest energy of the majority (minority)-spin conduction bands with respect to the Fermi level and the absolute value of the highest energy of the majority (minority)-spin valence bands [38, 39]. The half-metallic gap is located at Γ high symmetry point between the maximum of valence bands and Fermi level (E_F) for the $Ba_{0.75}Cr_{0.25}Se$ and $Ba_{0.5}Cr_{0.5}Se$, whereas it occurs between E_F and minimum of conduction bands for $Ba_{0.25}Cr_{0.75}Se$. Table 2 shows the calculated indirect band gap ($E^{\Gamma-X}$) of BaSe, half-metallic gaps (G_{HMF}) and half-metallic gaps (G_{HM}) of $Ba_{1-x}Cr_xSe$ with other theoretical [29–33], and experimental [40, 41] results. The predicted indirect band gap of BaSe is in good agreement with theoretical calculations [31, 33], while it is far than that of the experimental values [40, 41] because GGA approach underestimates the band gap [42–44]. For the $Ba_{1-x}Cr_xSe$ compounds, we understand that the half-metallic ferromagnetic decreases with in increasing concentration of chromium atom due to broadening of 3d levels of Cr around E_F.

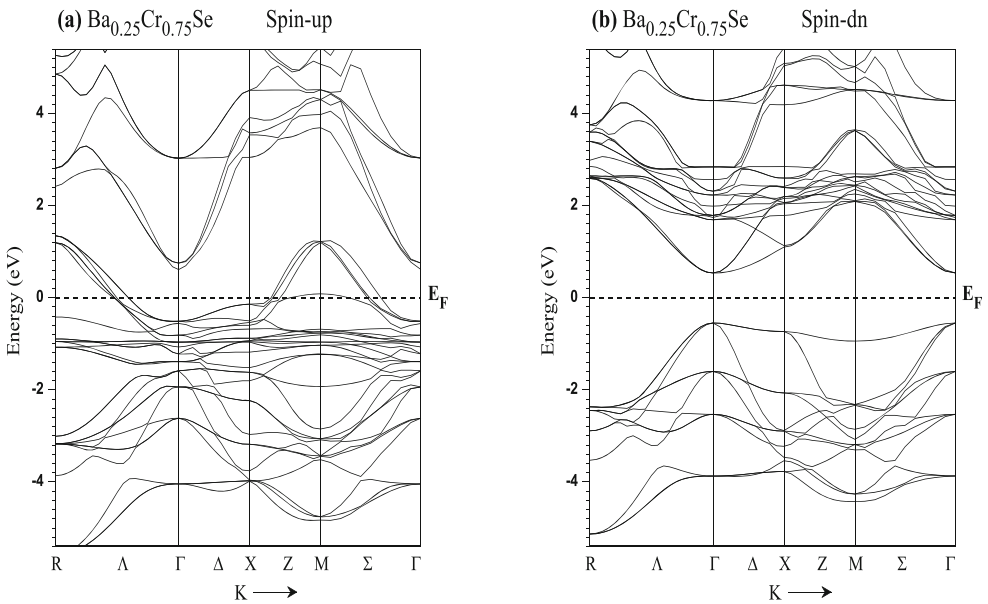

Fig. 4 Spin-polarized band structures for $Ba_{0.25}Cr_{0.75}Se$. **a** Majority spin (up) and **b** minority spin (dn). The Fermi level is set to zero (horizontal dotted line)

Table 2 Calculated indirect band gap ($E^{\Gamma\ X}$) for BaSe, half-metallic ferromagnetic gap (G_{HMF}), and half-metallic gap (G_{HM}) of minority-spin bands for $Ba_{1-x}Cr_xSe$ at concentrations $x = 0.25$, 0.5, and 0.75

Compound	G_{HMF} (eV)	G_{HM} (eV)	$E^{\Gamma\ X}$ (eV)	Method	Behavior
This work				GGA-WC	
BaSe			1.843		
$Ba_{0.75}Cr_{0.25}Se$	1.832	0.300			HMF
$Ba_{0.5}Cr_{0.5}Se$	1.668	0.501			HMF
$Ba_{0.25}Cr_{0.75}Se$	1.084	0.536			HMF
Other calculations					
BaSe			1.680 [29], 2.015 [30], 1.812 [31]	GGA-WC	
			2.028 [32], 1.986 [33]	GGA-PBE	
			3.58 [40], 3.6 [41]	Experimental	

To explain the origin of half-metallic character in $Ba_{1-x}Cr_xSe$, we have investigated the contribution of densities of states (DOS) around the Fermi level (E_F). Figures 5, 6, and 7 illustrate the spin-polarized total and partial densities of states for $Ba_{0.75}Cr_{0.25}Se$, $Ba_{0.5}Cr_{0.5}Se$, and $Ba_{0.25}Cr_{0.75}Se$, respectively. The DOS of majority-spin states for all compounds

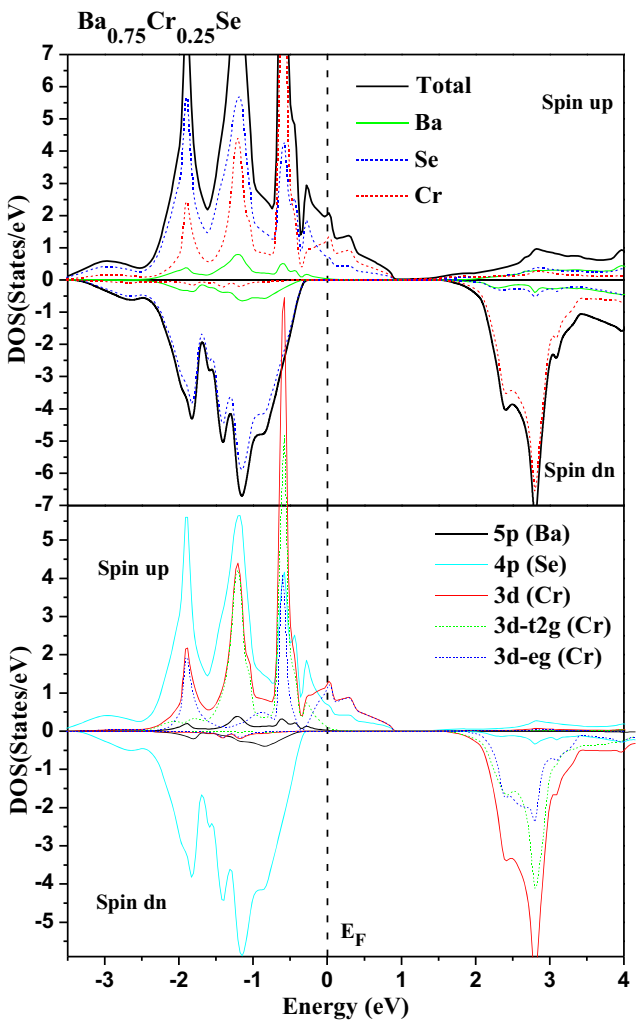

Fig. 5 Spin-polarized total and partial DOS of (5p) of Ba, (4p) of Se, and (3d, 3d-t_{2g}, and 3d-e_g) of Cr atoms in supercell of $Ba_{0.75}Cr_{0.25}Se$. The Fermi level is set to zero (vertical dotted line)

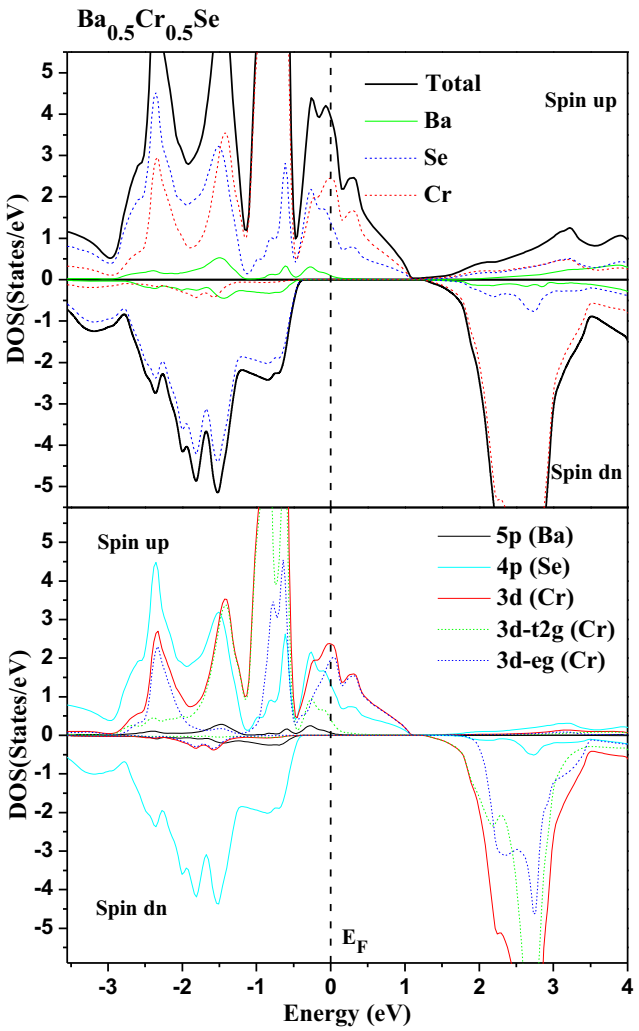

Fig. 6 Spin-polarized total and partial DOS of (5p) of Ba, (4p) of Se, and (3d, 3d-t_{2g}, and 3d-e_g) of Cr atoms in supercell of $Ba_{0.5}Cr_{0.5}Se$. The Fermi level is set to zero (vertical dotted line)

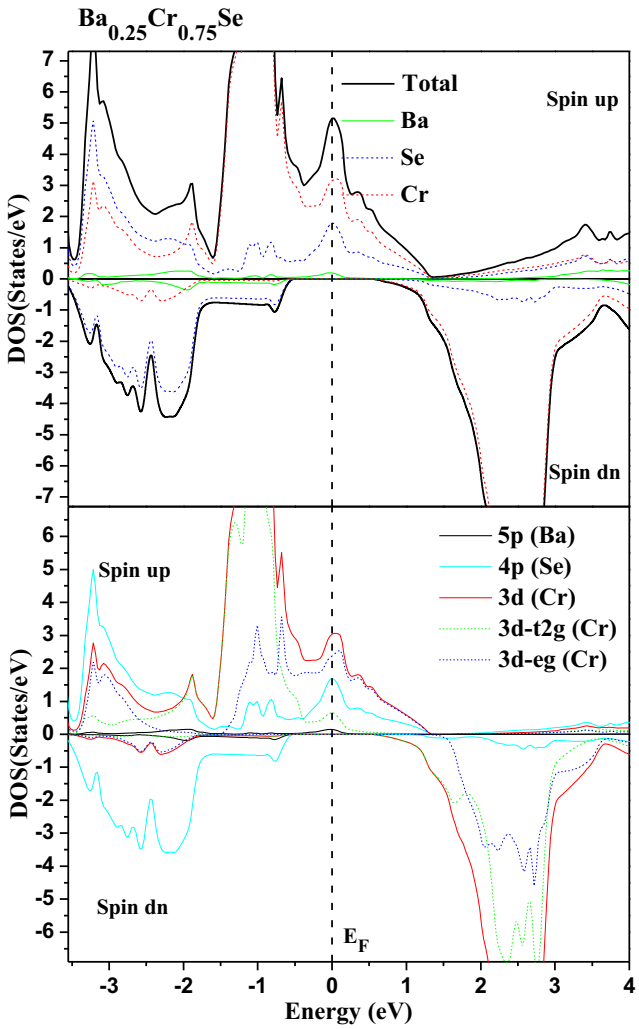

Fig. 7 Spin-polarized total and partial DOS of (5p) of Ba, (4p) of Se, and (3d, 3d-t_{2g}, and 3d-e_g) of Cr atoms in supercell of $Ba_{0.25}Cr_{0.75}Se$. The Fermi level is set to zero (vertical dotted line)

are metallic due to strong p-d hybridization between the p(Se) and d(Cr) levels. Simultaneously, the minority-spin channel does not have density of states at E_F. Moreover, the contribution of the DOS of spin up and spin down around E_F describes the spin polarization (P) of material, which can be determined by the following expression [45]:

$$P = \frac{N\uparrow(E_F) - N\downarrow(E_F)}{N\uparrow(E_F) + N\downarrow(E_F)}\ 100 \tag{2}$$

Table 3 Calculated total and local magnetic moments per Cr atom of the relevant Cr, Ba, and Se atoms and in the interstitial sites (in Bohr magneton μ_B) for $Ba_{1-x}Cr_xSe$ at concentrations $x = 0.25$, 0.5, and 0.75

Compound	Total (μ_B)	Cr (μ_B)	Ba (μ_B)	Se (μ_B)	Interstitial (μ_B)
$Ba_{0.75}Cr_{0.25}Se$	4	3.911	0.003	−0.144	0.233
$Ba_{0.5}Cr_{0.5}Se$	4	3.884	0.004	−0.218	0.331
$Ba_{0.25}Cr_{0.75}Se$	4	3.827	−0.002	−0.159	0.336

where the $N\uparrow(E_F)$ and $N\downarrow(E_F)$ are the DOS of majority spin and minority spin around Fermi level, respectively. We have found that the spin polarization $P = 1$ for $Ba_{1-x}Cr_xSe$ compounds at all concentrations, resulting from metallic nature of majority spin and semiconductor feature of minority spin. We have understand from our findings of electronic structures that the $Ba_{0.75}Cr_{0.25}Se$, $Ba_{0.5}Cr_{0.5}Se$, and $Ba_{0.25}Cr_{0.75}Se$ materials are half-metallic ferromagnetic with a spin polarization of 100%, which make them promising candidates for spintronics applications.

Furthermore, we have calculated the total and local magnetic moments per Cr atom of relevant Ba, Cr, and Se atoms, and at interstitial site of $Ba_{1-x}Cr_xSe$ doping systems. Table 3 depicts that the total magnetic moment for each compound is integral Bohr magneton of 4 μ_B, which is principally formed by the local magnetic moment of the Cr atom. The total magnetic moment of 4 μ_B is originated from the partially filled 3d (Cr) majority-spin states with four electrons. The large p–d exchange interaction reduces the predicted magnetic moment of 3d (Cr) less than 4 μ_B and induces minor magnetic moments at Ba, Se, and interstitial sites. Besides, the positive magnetic moments of Cr and Ba atoms for $Ba_{0.75}Cr_{0.25}Se$, $Ba_{0.5}Cr_{0.5}Se$ materials, lead to the ferromagnetic interaction between Cr and Ba, but the anti-ferromagnetic interaction is explained by the opposite magnetic signs of Cr and Se atoms.

We have used the band structures to calculate important factors such as the p–d exchange splitting $\Delta_x^v(pd) = E_v^{\downarrow} - E_v^{\uparrow}$ and $\Delta_x^c(pd) = E_c^{\downarrow} - E_c^{\uparrow}$, and the s–d exchange constants $N_0\alpha$ (conduction band) and the p–d exchange constants $N_0\beta$ (valence band). The $N_0\alpha$ and $N_0\beta$ parameters are calculated from the mean-field theory by the use of the following expressions [46, 47]:

$$N_0\alpha = \frac{\Delta E_c}{x\,\langle s\rangle} \tag{3}$$

$$N_0\beta = \frac{\Delta E_v}{x\,\langle s\rangle} \tag{4}$$

where the $\Delta E_c = E_c^{\downarrow} - E_c^{\uparrow}$ is the conduction band-edge spin-splittings and the $\Delta E_v = E_v^{\downarrow} - E_v^{\uparrow}$ is the valence band-edge spin-splittings of $Ba_{1-x}Cr_xSe$ at Γ high symmetry point. The $\langle s\rangle$ is the half total magnetic moment per Cr atom [46], and the x is the concentration of Cr impurity.

The computed p–d exchange splitting and exchange constants are given in Table 4. The positive $N_0\alpha$ constant suggests the ferromagnetic coupling between the 3d states of chromium (Cr) and conduction bands. The $\Delta_x^v(pd)$ and $\Delta_x^c(pd)$ parameters determine the attraction nature in the $Ba_{1-x}Cr_xSe$. However, the negative $\Delta_x^v(pd)$ of $Ba_{1-x}Cr_xSe$ at all concentrations means that the potential of minority spin is effective compared to the majority spin [48], this is an important property of spin-polarized materials [48, 49].

Table 4 Calculated p–d exchange splitting $\Delta_x^v(pd) = E_v^{\downarrow} - E_v^{\uparrow}$ and $\Delta_x^c(pd) = E_c^{\downarrow} - E_c^{\uparrow}$, and exchange constants $N_0\alpha$ and $N_0\beta$ for $Ba_{1-x}Cr_xSe$ at concentrations $x = 0.25$, 0.5, and 0.75

Compound	$\Delta_x^c(pd)$ (eV)	$\Delta_x^v(pd)$ (eV)	$N_0\alpha$	$N_0\beta$
$Ba_{0.75}Cr_{0.25}Se$	1.173	− 0.031	2.344	− 0.062
$Ba_{0.5}Cr_{0.5}Se$	0.864	− 0.052	0.864	− 0.052
$Ba_{0.25}Cr_{0.75}Se$	− 0.073	− 0.035	− 0.049	− 0.023

4 Conclusion

The DFT based on the FP-LAPW method is used to calculate the structural, electronic, and magnetic properties of $Ba_{1-x}Cr_xSe$ at concentrations $x = 0.25$, 0.50, and 0.75. We have employed the GGA-WC exchange and correlation potential to predict the structural parameters, the spin-polarized band structures and densities of states. The results of lattice constant and indirect band gap of BaSe are in good agreement with theoretical calculations. The electronic structures of $Ba_{1-x}Cr_xSe$ compounds show a half-metallic behavior for all concentrations x. The half-metallic character around Fermi level of $Ba_{1-x}Cr_xSe$ results from the strong p–d hybridization of majority spin and a gap of minority spin, leading to spin polarization of 100%. The total magnetic moments are 4 μ_B confirm both ferromagnetic nature and half-metallic behavior of $Ba_{1-x}Cr_xSe$ doping compounds. Therefore, the $Ba_{1-x}Cr_xSe$ materials seem to be promising candidates for possible spintronics applications. From our knowledge, there are no previous theoretical or experimental studies on the $Ba_{1-x}Cr_xSe$ materials; thus, we hope that our results serve as a reference for future theoretical and experimental researches.

References

1. Sato, K., Katayama-Yoshida, H.: Material design of GaN-based ferromagnetic diluted magnetic semiconductors. Jpn. J. Appl. Phys. **40**, L485–L487 (2001)
2. Wolf, S.A., Awschalom, D.D., Buhrman, R.A., Daughton, J.M., von Molnár, S., Roukes, M.L., Chtchelkanova, A.Y., Treger, D.M.: Spintronics: a spin-based electronics vision for the future. Science. **294**, 1488–1495 (2001)
3. Doumi, B., Tadjer, A., Dahmane, F., Mesri, D., Aourag, H.: Investigations of structural, electronic, and half-metallic ferromagnetic properties in (Al, Ga, in)$_{1-x}$M$_x$N (M = Fe, Mn) diluted magnetic semiconductors. J. Supercond. Nov. Magn. **26**, 515–525 (2013)
4. Doumi, B., Mokaddem, A., Temimi, L., Beldjoudi, N., Elkeurti, M., Dahmane, F., Sayede, A., Tadjer, A., Ishak-Boushaki, M.: First-principle investigation of half-metallic ferromagnetism in octahedrally bonded Cr-doped rock-salt SrS, SrSe, and SrTe. Eur. Phys. J. B. **88**, 93 (2015)
5. Berber, M., Doumi, B., Mokaddem, A., Mogulkoc, Y., Sayede, A., Tadjer, A.: Investigation of electronic structure and half-metallic ferromagnetic behavior with large half-metallic gap in $Sr_{1-x}V_xO$. J. Comput. Electron. **16**, 542–547 (2017)
6. Matsukura, F., Tokura, Y., Ohno, H.: Control of magnetism by electric fields. Nat. Nanotechnol. **10**, 209–220 (2015)
7. Nie, T., Tang, J., Wang, K.L.: Quest for high-Curie temperature Mn_xGe_{1-x} diluted magnetic semiconductors for room temperature spintronics applications. J. Cryst. Growth. **425**, 279–282 (2015)
8. Kaminska, M., Twardowski, A., Wasik, D.: Mn and other magnetic impurities in GaN and other III–V semiconductors-perspective for spintronic applications. J. Mater. Sci. Mater. Electron. **19**, 828–834 (2008)
9. Verma, U.P., Devi, N., Sharma, S., Jensen, P.: Spin-polarized first-principles study of ferromagnetism in zinc-blende $In_{1-x}Mn_xSb$. Eur. Phys. J. B. **81**, 381–386 (2011)
10. Rahman, G., Cho, S., Hong, S.C.: Half metallic ferromagnetism of Mn doped AlSb: a first principles study. Phys. Status Solidi B. **244**, 4435–4438 (2007)
11. Zerouali, A., Mokaddem, A., Doumi, B., Dahmane, F., Elkeurti, M., Sayede, A., Tadjer, A.: First-principle calculations of electronic and ferromagnetic properties of $Al_{1-x}V_xSb$. J. Comput. Electron. **15**, 1255–1262 (2016)
12. Yu, K.M., Walukiewicz, W.: Effect of the location of Mn sites in ferromagnetic $Ga_{1-x}Mn_xAs$ on its Curie temperature. Phys. Rev. B. **201303**(R), 65 (2002)
13. Jungwirth, T., Sinova, J., Mašek, J., Kučera, J., MacDonald, A.H.: Theory of ferromagnetic (III,Mn)V semiconductors. Rev. Mod. Phys. **78**, 809–864 (2006)
14. Akhtar, M.S., Malik, M.A., Riaz, S., Naseem, S.: Room temperature ferromagnetism and half metallicity in nickel doped ZnS: experimental and DFT studies. Mater. Chem. Phys. **160**, 440–446 (2015)
15. Akhtar, M.S., Malik, M.A., Alghamdi, Y.G., Ahmad, K.S., Riaz, S., Naseem, S.: Chemical bath deposition of Fe-doped ZnS thin films: investigations of their ferromagnetic and half-metallic properties. Mater. Sci. Semicond. Process. **39**, 283–291 (2015)
16. Tian, J.H., Song, T., Sun, X.W., Wang, T., Jiang, G.: First-principles study on the half-metallic ferromagnetism and optical properties of Fe-doped CdSe and co-doped CdSe. J. Supercond. Nov. Magn. **30**, 521–528 (2017)
17. Rabbani, S.F., Banu, I.B.S.: An ab-initio calculation of halfmetallic ferromagnetism in vanadium doped ZnS. J. Alloys Compd. **695**, 3131–3138 (2017)
18. Addadi, Z., Doumi, B., Mokaddem, A., Elkeurti, M., Sayede, A., Tadjer, A., Dahmane, F.: Electronic and ferromagnetic properties of 3d(V)-doped (BaS) barium sulfide. J. Supercond. Nov. Magn. **30**, 917–923 (2017)
19. Berber, M., Doumi, B., Mokaddem, A., Mogulkoc, Y., Sayede, A., Tadjer, A.: First-principle predictions of electronic properties and half-metallic ferromagnetism in vanadium-doped rock-salt SrO. J. Electron. Mater. **47**, 449–456 (2018)
20. Kohn, W., Sham, L.J.: Self-consistent equations including exchange and correlation effects. Phys. Rev. **140**, A1133–A1138 (1965)
21. Wu, Z., Cohen, R.E.: More accurate generalized gradient approximation for solids. Phys. Rev. B. **73**(235116), 1–6 (2006)
22. Blaha, P., Schwarz, K., Madsen, G.K.H., Kvasnicka, D., Luitz, J.: WIEN2k, an augmented plane wave plus local orbitals program for calculating crystal properties. Vienna University of Technology, Vienna (2001)
23. Monkhorst, H.J., Pack, J.D.: Special points for Brillonin-zone integrations. Phys. Rev. B. **13**, 5188–5192 (1976)
24. Pack, J.D., Monkhorst, H.J.: "Special points for Brillonln-zone integrations"—a reply. Phys. Rev. B. **16**, 1748–1749 (1977)
25. Slattery, M.K.: The crystal structure of metallic tellurium and selenium and of strontium and barium selenide. Phys. Rev. **25**, 333–337 (1925)

26. Bai, J., Raulot, J.-M., Zhang, Y., Esling, C., Zhao, X., Zuo, L.: The effects of alloying element Co on Ni–Mn–Ga ferromagnetic shape memory alloys from first-principles calculations. Appl. Phys. Lett. **98**, 164103 (2011)
27. Doumi, B., Mokaddem, A., Ishak-Boushaki, M., Bensaid, D.: First-principle investigation of magnetic and electronic properties of vanadium- and chromium-doped cubic aluminum phosphide. Mater. Sci. Semicond. Process. **32**, 166–171 (2015)
28. Muranghan, F.D.: The compressibility of media under extreme pressures. Proc. Natl. Acad. Sci. U. S. A. **30**, 244–247 (1944)
29. Bhattacharjee, R., Chattopadhyaya, S.: Effects of barium (Ba) doping on structural, electronic and optical properties of binary strontium chalcogenide semiconductor compounds—a theoretical investigation using DFT based FP-LAPW approach. Mater. Chem. Phys. **199**, 295–312 (2017)
30. Chattopadhyaya, S., Bhattacharjee, R.: Theoretical study of structural, electronic and optical properties of $Ba_xPb_{1-x}S$, $Ba_xPb_{1-x}Se$ and $Ba_xPb_{1-x}Te$ ternary alloys using FP-LAPW approach. J. Alloys Compd. **694**, 1348–1364 (2017)
31. Bhattacharjee, R., Chattopadhyaya, S.: Theoretical investigation of structural, electronic and optical properties of $Mg_xBa_{1-x}S$, $Mg_xBa_{1-x}Se$ and $Mg_xBa_{1-x}Te$ ternary alloys using DFT based FP-LAPW approach. J. Phys. Chem. Solids. **110**, 15–29 (2017)
32. Drablia, S., Boukhris, N., Boulechfar, R., Meradji, H., Ghemid, S., Ahmed, R., Bin Omran, S., El Haj Hassan, F., Khenata, R.: Ab initio calculations of the structural, electronic, thermodynamic and thermal properties of $BaSe_{1-x}$ Te_x alloys. Phys. Scr. **105701**(8pp), 92 (2017)
33. Nejatipour, H., Dadsetani, M.: Excitonic effects in the optical properties of alkaline earth chalcogenides from first-principles calculations. Phys. Scr. **085802**(16pp), 90 (2015)
34. Grzybowski, T.A., Ruoff, A.L.: High-pressure phase transition in BaSe. Phys. Rev. B. **27**, 6502–6503 (1983)
35. Kaneko, Y., Morimoto, K.T.: Optical properties of alkaline-earth chalcogenides. I. Single crystal growth and infrared reflection spectra due to optical phonons. J. Phys. Soc. Jpn. **51**, 2247–2254 (1982)
36. Ruoff, A.L., Grzybowski, T.A.: In: Minomura, S. (ed.) Solid state physics under pressure. Terra Scientific, Tokyo (1985)
37. Perdew, J.P., Burke, K., Ernzerhof, M.: Generalized gradient approximation made simple. Phys. Rev. Lett. **77**, 3865–3868 (1996)
38. Yao, K.L., Gao, G.Y., Liu, Z.L., Zhu, L.: Half-metallic ferromagnetism of zinc-blende CrS and CrP: a first-principles pseudopotential study. Solid State Commun. **133**, 301–304 (2005)
39. Gao, G.Y., Yao, K.L., Şaşıoğlu, E., Sandratskii, L.M., Liu, Z.L., Jiang, J.L.: Half-metallic ferromagnetism in zinc-blende CaC, SrC, and BaC from first principles. Phys. Rev. B. **75**, 174442 (2007)
40. Zolweg, R.J.: Optical absorption and photoemission of barium and strontium oxides, sulfides, seleniums, and tellurides. Phys. Rev. **111**, 113–119 (1958)
41. Saum, G.A., Hensley, E.B.: Fundamental optical absorption in the IIA-VIB compounds. Phys. Rev. **113**, 1019–1022 (1959)
42. Godby, R.W., Schlüter, M., Sham, L.J.: Accurate exchange-correlation potential for silicon and its discontinuity on addition of an electron. Phys. Rev. Lett. **56**, 2415–2418 (1986)
43. Rinke, P., Qteish, A., Neugebauer, J., Freysoldt, C., Scheffler, M.: Combining GW calculations with exact-exchange density-functional theory: an analysis of valence-band photoemission for compound semiconductors. New J. Phys. **7**, 126–126 (2005)
44. Rinke, P., Qteish, A., Neugebauer, J., Scheffler, M.: Exciting prospects for solids: exact-exchange based functionals meet quasiparticle energy calculations. Phys. Status Solidi B. **245**, 929–945 (2008)
45. Soulen Jr., R.J., Byers, J.M., Osofsky, M.S., Nadgorny, B., Ambrose, T., Cheng, S.F., Broussard, P.R., Tanaka, C.T., Nowak, J., Moodera, J.S., Barry, A., Coey, J.M.D.: Measuring the spin polarization of a metal with a superconducting point contact. Science. **282**, 85–88 (1998)
46. Sanvito, S., Ordejon, P., Hill, N.A.: First-principles study of the origin and nature of ferromagnetism in $Ga_{1-x}Mn_xAs$. Phys. Rev. B. **63**, 165206 (2001)
47. Raebiger, H., Ayuela, A., Nieminen, R.M.: Intrinsic hole localization mechanism in magnetic semiconductors. J. Phys. Condens. Matter. **16**, L457–L462 (2004)
48. Verma, U.P., Sharma, S., Devi, N., Bisht, P.S., Rajaram, P.: Spin-polarized structural, electronic and magnetic properties of diluted magnetic semiconductors $Cd_{1-x}Mn_xTe$ in zinc blende phase. J. Magn. Magn. Mater. **323**, 394–399 (2011)
49. Morozzi, V.L., Janak, J.F., Williams, A.R.: Calculated electronic properties of metals. Pergamon, New York (1978)